

# PCCP

Physical Chemistry Chemical Physics

Accepted Manuscript

This article can be cited before page numbers have been issued, to do this please use: P. Capera-Aragones, K. Matange, V. Rajaei, Y. Pinter, A. S. Petrov, L. D. Williams and M. Frenkel Pinter, *Phys. Chem. Chem. Phys.*, 2026, DOI: 10.1039/D5CP03057A.



This is an Accepted Manuscript, which has been through the Royal Society of Chemistry peer review process and has been accepted for publication.

Accepted Manuscripts are published online shortly after acceptance, before technical editing, formatting and proof reading. Using this free service, authors can make their results available to the community, in citable form, before we publish the edited article. We will replace this Accepted Manuscript with the edited and formatted Advance Article as soon as it is available.

You can find more information about Accepted Manuscripts in the [Information for Authors](#).

Please note that technical editing may introduce minor changes to the text and/or graphics, which may alter content. The journal's standard [Terms & Conditions](#) and the [Ethical guidelines](#) still apply. In no event shall the Royal Society of Chemistry be held responsible for any errors or omissions in this Accepted Manuscript or any consequences arising from the use of any information it contains.

# Stringent Selection on Kinetics of Condensation Reactions: Early Steps in Chemical Evolution

Pau Capera-Aragones<sup>a,b,c</sup>, Kavita Matange<sup>a,b</sup>, Vahab Rajaei<sup>a,b</sup>, Yuval Pinter<sup>d</sup>, Anton S Petrov<sup>a,b</sup>, Loren Dean Williams<sup>a,b\*</sup>, and Moran Frenkel-Pinter<sup>b,c,e\*</sup>

<sup>a</sup> NASA Center for the Origins of Life, Georgia Institute of Technology, Atlanta, GA 30332-0400

<sup>b</sup> School of Chemistry and Biochemistry Georgia Institute of Technology, 315 Ferst Drive NW, Atlanta, GA 30332-0400

<sup>c</sup> Institute of Chemistry, The Hebrew University of Jerusalem, Edmond J. Safra Campus, Jerusalem 9190401, Israel

<sup>d</sup> Department of Computer Science, Ben-Gurion University of the Negev, Israel

<sup>e</sup> Blue Marble Space Institute of Science, Seattle, WA 98104, USA

\*Co-corresponding authors

\*Corresponding Authors:

Dr. Moran Frenkel-Pinter

The Center for Nanoscience and Nanotechnology  
Institute of Chemistry  
The Hebrew University of Jerusalem  
Edmond J. Safra Campus  
Jerusalem 9190401, Israel  
Ph: (+972)-2-6584171  
*moran.fp@mail.huji.ac.il*

Dr. Loren Dean Williams

School of Chemistry and Biochemistry  
Georgia Institute of Technology  
315 Ferst Drive NW  
Atlanta, GA 30332-0400  
Ph: (+1) (404) 385-6258  
*loren.williams@chemistry.gatech.edu*

**Keywords:** Origins of life, Prebiotic chemistry, Chemical evolution, Compression, Water Chemistry

## Abstract

The emergence of chemical selectivity poses a central challenge in origins-of-life research. As demonstrated by analyses of asteroid and meteorite samples, abiotic chemistry is incredibly messy. Experiments show that even limited sets of reactive species can undergo vast numbers of distinct chemical transformations, leading to a combinatorial explosion of products. These explosions arise from the numerous ways in which reactants in mixtures can combine, generating large and chemically diverse ensembles that reduce or even preclude the possibility of productive pathways of chemical evolution. However, recent empirical studies have demonstrated that under kinetic control, chemical systems can exhibit combinatorial compression—a marked reduction in product diversity relative to combinatorial expectations. This selective phenomenon is observed under conditions of low water activity, such as in the dry phase of wet–dry cycling experiments. Here, we integrate transition-state theory with computer simulations to demonstrate that experimentally observed combinatorial compression is a consequence of kinetic selection in condensation–dehydration reactions. Kinetic selection depends on several key factors: (i) chemical connectivity, where multiple species can react with each other; (ii) at least one particularly reactive species—termed a “kinetic compressor”; and (iii) appropriate temperature, concentrations, and reaction times. We find that small differences in activation free energies, on the order of just  $\sim$ 3 kcal/mol, can dominate a kinetic landscape, dramatically limiting product distributions. Connected systems can favor a narrow subset of products, suggesting selection mechanisms in prebiotic contexts. Our results provide mechanistic insight into combinatorial compression, establish a quantitative framework for exploring the emergence of stringent chemical selectivity, and can guide future experimental efforts in chemical evolution.

## Introduction

Geochemical and environmental processes on the ancient Earth gave rise to biology by processes that are poorly understood. Increasing complexity of large molecules (1), accompanied by a reduction in chemical diversity, ultimately favored a small set of building blocks that now compose the universal biopolymers – RNA, DNA, proteins, and glycans (2). Recognizing that spontaneous, unguided processes in natural environments produced the remarkable molecules of life can inspire exploration of new frontiers in chemistry.

Key insights into the origins of biopolymers have come from considering the effects of oscillating water activity. The rotation of Earth (diurnal cycle) induces daily wet and dry phases, with surfaces wetting at night and drying during the day (3, 4). Such wet–dry cycling causes systematic alterations in the driving forces of reactions involving water as a reactant or product. Dry phases promote condensation–dehydration reactions and the formation of oligomers, while wet phases favor hydrolysis and the breakdown of oligomers.

It has been demonstrated that when diverse mixtures of mercapto acids, hydroxy acids, and amino acids are concentrated at low water activity, they can form interconnected reaction networks with emergent behaviors (5–13). Emergent behaviors are those not predicted by the properties of isolated components (14). One such emergent behavior is combinatorial compression. Experiments have shown that wet–dry cycling at modest temperatures imposes chemical selection, favoring a limited set of products from many possible reaction outcomes (12, 13).



*Combinatorial compression* is the production of small numbers of products, representing only a small fraction of what is theoretically possible (Figure 1). Under experimental conditions of combinatorial compression, reinitiation of a reaction with additional (new) reactants led to the disappearance of previous products (product subtraction) and the appearance of new products, without combinatorial increase in the total number of products (Figure 1). Addition of new reactants causes product identities to shift but does not significantly increase product counts. This effect is observed at relatively low temperatures (45°C) but not at higher temperatures (85°C), where selection collapses and products proliferate (*combinatorial explosion* (15-19)). As reaction temperature increases, a system transitions from combinatorial compression to combinatorial explosion (12).

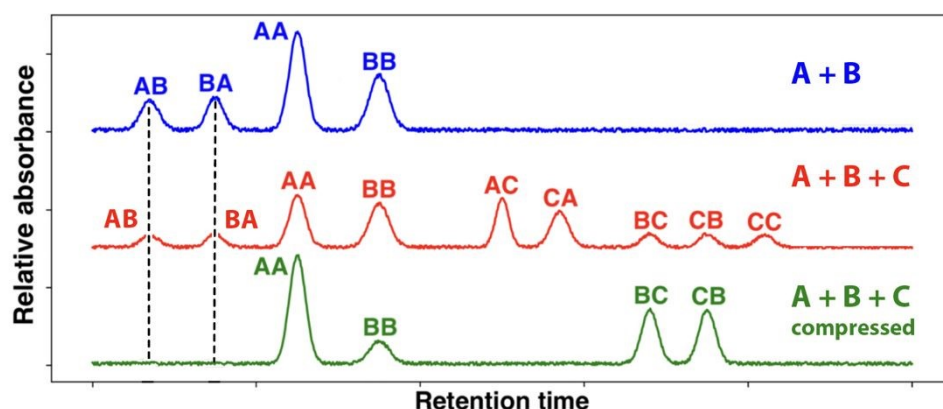


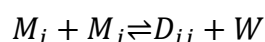
**Figure 1.** A schematic representation of combinatorial compression in a UV-Vis HPLC chromatogram of products of dry-down reactions as previously published (12). Each peak here corresponds to a dimer product. Top: two monomers A and B combine to form four dimers, AB, BA, AA, and BB. Middle: three monomers A, B, and C combine to form nine dimers under conditions of combinatorial explosion. Bottom: Three monomers, A, B, and C combine to form four dimers under conditions of combinatorial compression. Combinatorial compression is represented by the absence of dimers AB, BA, AC, CA and CC. Product subtraction is indicated by vertical dashed lines.

Although combinatorial compression has been observed experimentally (12), it has not yet been addressed theoretically, and its mechanistic basis remains unknown. Here, we integrate transition state theory with computer simulations and demonstrate that experimentally observed combinatorial compression is a consequence of kinetic selection in condensation-dehydration reactions and depends on several key factors: (i) chemical connectivity, where multiple species can react with each other, (ii) a particularly reactive species – termed a ‘compressor’, and (iii) appropriate temperature, concentrations and reaction time. We find that small differences in activation free energies, on the order of just 3-5 kcal/mol, can dominate a kinetic landscape, dramatically limiting product distributions. The terms compressor and chemical connectivity are defined more fully in subsequent sections. A mechanistic explanation for combinatorial compression enables new experimental and theoretical strategies for driving the evolution of complex chemical mixtures. These findings have implications for the origins of life, systems chemistry, and dynamic combinatorial chemistry (20-23).

## Results

### Combinatorial Compression under Kinetic Control

**The Model.** Our simulations are based on reversible condensation-dehydration reactions between monomers:



where  $M_i$  and  $M_j$  are monomers,  $D_{ij}$  is their covalent dehydrated dimer product, and  $W$  is water. Coupled ordinary differential equations describing these reactions are solved numerically to obtain time-dependent concentrations of all species. Simulations are conducted at low water activity, corresponding to the dry phase of wet-dry cycling, where monomer and dimer concentrations are relatively high and water concentration is held constant at a low value. We restrict reactions to monomer-dimer interconversion; trimers and larger oligomers are excluded. A dimer is considered a reaction product if its concentration exceeds a detection threshold.

The kinetic and thermodynamic parameters (Table 1) are similar to those of known prebiotic reactions (24) but do not represent exact values for any specific system. To capture the inherent variability of chemical processes in mixtures, each parameter is defined by a mean and standard deviation. We examine system behavior across a range of parameter values to identify conditions that produce combinatorial compression.

Simulations are run in two modes: kinetic (finite time intervals) and thermodynamic (equilibrium, no time constraint). We assume homogeneous systems with negligible diffusion limitations (25), constant activity coefficients, and constant pH. Temperature dependencies of enthalpy and entropy are neglected, and entropy contributions are assumed to be small, such that reaction free energies are predominantly determined by enthalpy. At most one compressor species is present in any simulation, though future work will explore multiple compressors. Subsequent studies will expand the parameter space explored here.



Table 1. Summary of parameters and conditions used in the simulations

Parameter	Value
Number of monomers	12
[Water]	0.5 (M) <sup>1</sup>
[Monomer] <sub>initial</sub>	0.05 (M) <sup>1</sup>
[Dimer] <sub>initial</sub>	0 (M)
mean $\Delta G^\ddagger$	25 (kcal/mol) <sup>2</sup>
standard deviation of $\Delta G^\ddagger$ [ $\sigma(\Delta G^\ddagger)$ ]	0.289 (kcal/mol) <sup>3</sup>
mean $\Delta H_{rxn}^o$	8 (kcal/mol) <sup>2</sup>
standard deviation of $\Delta H_{rxn}^o$ [ $\sigma(\Delta H_{rxn}^o)$ ]	0.289 kcal/mol <sup>3</sup>
mean $\Delta S_{rxn}^o$	0.033 kcal/mol•K <sup>2</sup>
standard deviation of $\Delta S_{rxn}^o$ [ $\sigma(\Delta S_{rxn}^o)$ ]	0 kcal/mol•K <sup>3</sup>
mean $\Delta G_{rxn}$	-2.4 kcal/mol <sup>2</sup>
standard deviation of $\Delta G_{rxn}$ [ $\sigma(\Delta G_{rxn})$ ]	0.289 kcal/mol <sup>3</sup>
Concentration Threshold	$10^{-4}$ M <sup>4</sup>
Connectivity	fully connected <sup>5</sup>
Temperature	40 °C <sup>6</sup>
Time interval	1000 s <sup>7</sup>
Kinetic Compression	
[Kinetic Compressor] <sub>initial</sub>	2.5 M <sup>1</sup>
mean $\Delta G_{\text{kinetic compressor}}^\ddagger$	20 kcal/mol ( $\Delta\Delta G^\ddagger = -5$ kcal/mol) <sup>8</sup>
standard deviation $\sigma(\Delta G_{\text{kinetic compressor}}^\ddagger)$	0 kcal/mol <sup>3</sup>
Thermodynamic Compression	
[Thermodynamic Compressor] <sub>initial</sub>	25 M <sup>1</sup>
mean $\Delta H_{rxn, \text{thermodynamic compressor}}^o$	0 kcal/mol <sup>9</sup>
$\sigma(\Delta H_{rxn, \text{thermodynamic compressor}}^o)$	0 kcal/mol <sup>3</sup>
mean $\Delta G_{rxn, \text{thermodynamic compressor}}$	-10.4 kcal/mol <sup>10</sup> ( $\Delta\Delta G_{rxn} = -8$ kcal/mol)
$\sigma(\Delta G_{rxn, \text{thermodynamic compressor}})$	0 kcal/mol <sup>3</sup>

- 1) These simulations take place in the dry phase where the concentration of water is low, and the concentration of monomers is high. For the compressor, a range of initial concentrations was investigated. In some cases, the system was fed with a compressor, by holding its concentration constant at 0.05M.
- 2) The mean activation reaction free energy, and the standard enthalpy, entropy, and free energy of dimerization for reactions that do not involve the kinetic compressor. The free energy of reactions varies with temperature.
- 3) The standard deviation of the activation reaction free energy, and the standard enthalpy, entropy, and free energy of reactions that do not involve the kinetic compressor. The standard deviation is defined by a uniform random distribution within an interval centered on the mean. For the kinetic compressor, no variation is applied.
- 4) The concentration threshold is the minimum concentration required for a monomer or dimer to be considered present in the reaction mixture.



5) All monomers are assumed to be fully connected — they can react with each other — except for the kinetic and thermodynamic compressors, whose connectivity varies among three defined states: *fully connected*, *partially connected*, and *isolated*. A *fully connected* compressor can react with all other monomers to form dimers; a *partially connected* compressor reacts with only a subset of monomers; and an *isolated* compressor does not react with any.

6) Previous experiments have shown that this temperature is appropriate for combinatorial compression (12). For some simulations the variation of temperature is investigated.

7) Previous experiments have shown that this time interval is appropriate for combinatorial compression (12).

8) The mean activation free energy for dimerization reactions involving the kinetic compressor. For some simulations this parameter is varied.

9) The mean standard enthalpy of reactions involving the thermodynamic compressor. For some simulations this parameter is varied.

10) The mean of the free energy of reactions involving the thermodynamic compressor. This parameter varies with  $\Delta H^\circ(\text{rxn})$  and the temperature.

We compared computation with experiment to test the utility of our model and to define the rules governing combinatorial compression. We observed in simulations that combinatorial compression depends on thermodynamic and kinetic properties of monomers, concentrations, and on temperature and reaction time.

**Connectivity.** We define the connectivity of a monomer as the extent to which it can chemically combine with other monomers in a mixture (Figure 2). Two monomers are connected if they react to form a dimer. A monomer with high connectivity forms dimers with many other monomers; a monomer with low connectivity reacts with few other monomers. A monomer can be isolated, partially connected, or fully connected (Figure 2). An isolated monomer is not connected to other monomers (Figure 2a). A partially connected monomer is connected to some monomers but not others (Figure 2b). A fully connected monomer is connected to all other monomers (Figure 2c). A complex system can contain a continuum of monomers that range from isolated to fully connected.  $M_i$  can affect  $M_j$  even if they are not connected. For example, in Figure 2b,  $M_1$  is not connected to  $M_6$ , but reactions with  $M_1$  may deplete  $M_7$ ,  $M_3$ , or  $M_2$ , which are connected to  $M_6$ . Addition of  $M_1$  may cause disappearance of dimers of reactions of  $M_7$ ,  $M_3$ , or  $M_2$  with other monomers. Connectivity is context-dependent: a monomer may exhibit high connectivity in one mixture but low connectivity in another, depending on the identities of the other components.

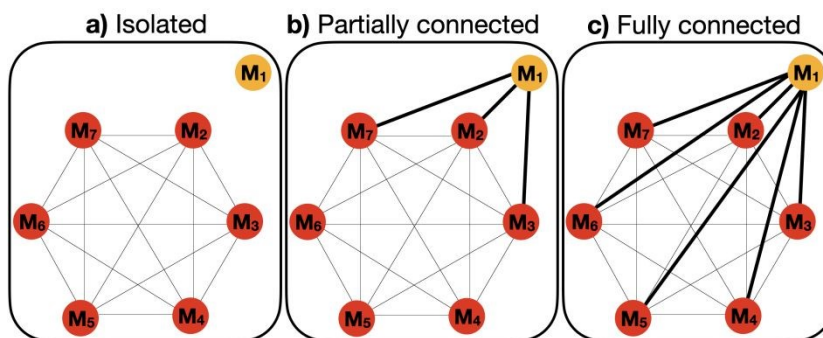


**Figure 2.** Schematic representation of chemical connectivity of monomer  $M_1$  in a mixture with  $M_2$ ,  $M_3$ ,  $M_4$ ,  $M_5$ ,  $M_6$ , and  $M_7$ . Our simulated mixtures contain 12 monomers. In this figure only 7 are represented for simplicity.  $M_i$  reacts with  $M_j$  to form dimers  $D_{ij}$  if a line links them. All  $M_i$  react with  $M_1$ . Monomers other than  $M_1$  are fully connected. Three levels of  $M_1$  connectivity are (a) isolated, (b) partially connected, and (c) fully connected.



**Kinetic Compression.** A kinetic compressor must be highly connected, at high concentration, and react at modest temperature with low activation energy ( $\Delta G^\ddagger$ ). The difference in  $\Delta G^\ddagger$  of the kinetic compressor compared to  $\Delta G^\ddagger$  of reactions between other monomers is -3 to -5 kcal/mol ( $\Delta\Delta G^\ddagger \approx -3$  to -5 kcal/mol, Figure 3). When a connected and a highly reactive monomer is at sufficient concentration, we call it a kinetic compressor ( $M_{kc}$ ), because it can depress populations of other dimers. If a small subset of reactions is significantly faster than others, the products of these reactions dominate the dimer mixture at appropriate time intervals. This definition assumes the system is under kinetic control, not thermodynamic control. A kinetic compressor is not a catalyst; it is chemically consumed during the reaction and does not stabilize a transition state. Although we have not yet simulated it, a catalyst could promote the activity of a given monomer, turning it into a kinetic compressor and contributing to compression.

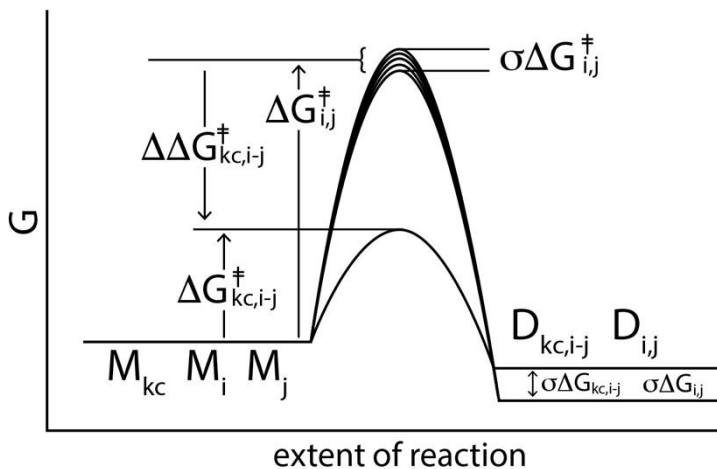


**Figure 3.** Schematic reaction coordinate for a system of connected monomers that react with each other and with a kinetic compressor ( $M_{kc}$ ).  $M_{kc}$  reacts with a relatively low activation free energy ( $\Delta\Delta G_{kc,i-j}^{\ddagger} < 0$ ) with other monomers. To better represent real chemical systems the simulation introduced small variations in activation free energies ( $\sigma\Delta G_{i,j}^{\ddagger}$ ) and in free energies of reaction ( $\sigma\Delta G_{i,j}$ ) and ( $\sigma\Delta G_{kc,i-j}$ ). At low temperature and appropriate concentrations, the rates of formation of dimers  $D_{kc,i-j}$  containing  $M_{kc}$  are greater than rates of formation of other dimers ( $D_{i,j}$ ).

**Effect of Concentration.** A kinetic compressor can constrain the number of observable dimers in a reactive mixture. We simulated dimerization reactions at various concentrations of kinetic compressors with a range of standard deviations in activation free energies of connected monomers (Figure 4). In the absence of a kinetic compressor, a connected mixture of twelve monomers undergoes combinatorial explosion, producing 144 dimers above the concentration threshold. A kinetic compressor induces kinetic compression, reducing the number of dimers that exceed the concentration threshold. As shown in Figure 4, increasing the concentration of the kinetic compressor causes a transition from combinatorial explosion to combinatorial compression; a kinetic compressor reduces the number of dimers that exceed the concentration threshold. At high compressor concentrations, the number of observed dimers is 23, corresponding to an 84% decrease in product diversity. The sharpness of transition depends on  $\sigma(\Delta G^\ddagger)$ , the standard deviation in activation free energies of dimerization reactions. Low deviation yields a sharp transition, while high deviation produces a gradual transition. When  $\sigma(\Delta G^\ddagger)$  is small, the kinetics of all reactions are similar, so they cross the concentration threshold nearly simultaneously, leading to a sharp transition.

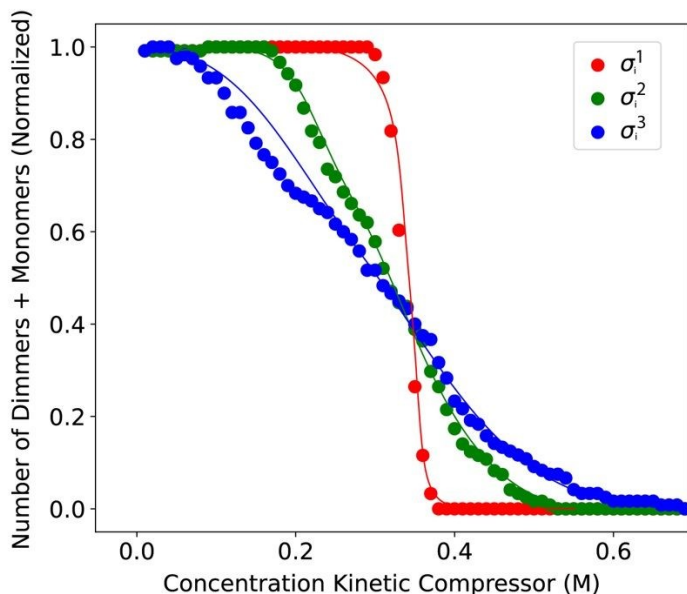


**Figure 4.** The number of dimers plus monomers above the concentration threshold depends on the concentration of the kinetic compressor and  $\sigma(\Delta G^\ddagger)$ , the standard deviation of the activation free energies. Parameters for this simulation are as indicated in Table 1, except for  $\sigma(\Delta G^\ddagger)$ , which is set to three different values:  $\sigma_i^1(\Delta G^\ddagger) = 0.043$  (red line),  $\sigma_i^2(\Delta G^\ddagger) = 0.213$  (green), or  $\sigma_i^3(\Delta G^\ddagger) = 0.340$  (blue) kcal/mol. Results are normalized from 0 to 1; values reaching the minimum appear as zero.

The concentration of kinetic compressor required to convert a system from combinatorial explosion to compression depends on the extent of connectivity,  $\Delta\Delta G^\ddagger$ , temperature, and the number and concentrations of monomers. Maintaining kinetic compression as the total concentration of non-compressing monomers increases requires a corresponding increase in the concentration of the kinetic compressor. This dependence arises because reaction fluxes are governed by aggregate encounter rates. The compressor competes not with a single species, but with the entire pool of non-compressing reactants: the total rate at which these species either react with the compressor or with each other scales with the sum of their concentrations. As a result, the effectiveness of kinetic compression is controlled by the ratio between the compressor concentration and the total concentration of competing reactants, rather than by any individual concentration alone. For the conditions in Table 1, an initial concentration of kinetic compressor  $> 0.3$  M is required to observe kinetic compression (Figure 4).

**Selection.** The simulations indicate how the number of monomers influences the number of dimer products in the presence or absence of a kinetic compressor (Figure 5). In the absence of a kinetic compressor, there is no selection and the system combinatorically explodes. The number of dimers increases with the square of the number of monomers. Six monomers produce 36 dimers. Twelve monomers produce 144 dimers. Twenty-five monomers produce 625 dimers. A kinetic compressor acts by effectively selecting certain reactions while excluding others. This selective behavior can cause the number of observed dimer products to increase linearly, rather than exponentially, with the number of reactant monomers. The linear relationship arises because the compressor selects reactions between itself and other monomers, suppressing reactions among alternative monomer pairs. In simulations of second order condensation reactions, the presence of a kinetic compressor reduces combinatorial diversity: for example, twenty-five monomers yield only forty-nine distinct dimers in the presence of a compressor. These results are consistent with experimental observations. In wet-dry cycling experiments using complex chemical mixtures (12), we found that, under certain conditions, the number of observable

products did not scale with the number of reactants as predicted by combinatorics. At relatively low temperatures, increasing the number of reactants changed the identities of products, but not their number.

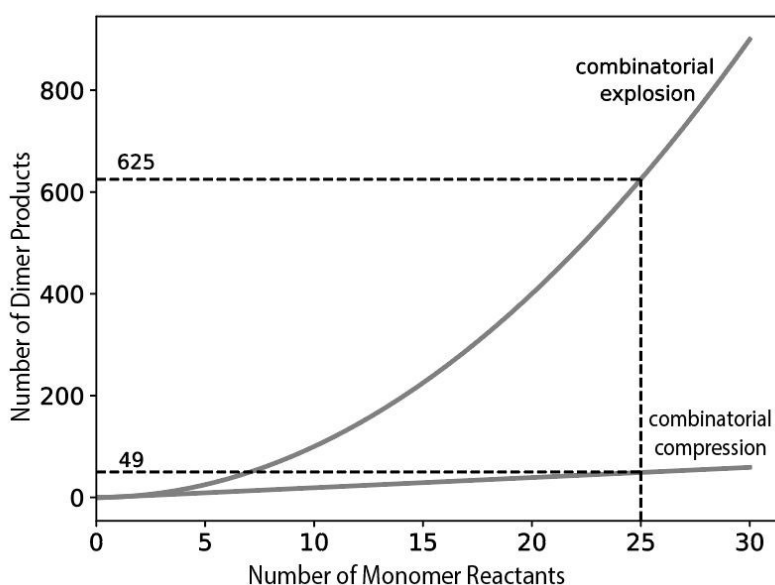


**Figure 5.** In the absence of a kinetic compressor, the number of product dimers above the concentration threshold increases exponentially with the number of reactant monomers. In the presence of a kinetic compressor, the number of dimers above the threshold increases linearly with the number of monomers. The reaction conditions are indicated in Table 1.

The simulations demonstrate how under specific conditions, addition of new monomers can systematically add new dimers and subtract other dimers from the product mixture. Figure 6a shows that in the absence of a kinetic compressor in a highly connected system, all dimers rise above the concentration threshold. This simulation corresponds to combinatorial explosion, as observed in Figure 5. However, reinitiating the reaction in the presence of a kinetic compressor leads to the emergence of a new set of dimers and the suppression of an existing set. The newly formed dimers contain the kinetic compressor linked to other monomers and are produced via fast reactions with low activation free energies. In contrast, the suppressed dimers arise from pairs of monomers that do not include the kinetic compressor and react with higher activation free energies. As a result, this latter set of dimers does not exceed the concentration threshold at the time point of measurement (Figure 6b). Chemical selection based on reaction rates therefore stems, in part, from the rapid consumption of certain monomers by the kinetic compressor. These quickly consumed reactants are unavailable for other reactions, subtracting products from the reaction mixture. Our simulations demonstrate that product subtraction by a kinetic compressor is more pronounced when the kinetic compressor reacts at lower reaction free energy (greater negative  $\Delta\Delta G^\ddagger$ ) (Figure S1). We observe resilience in production of some dimers that are not connected to the compressor and are not subtracted by the compressor.



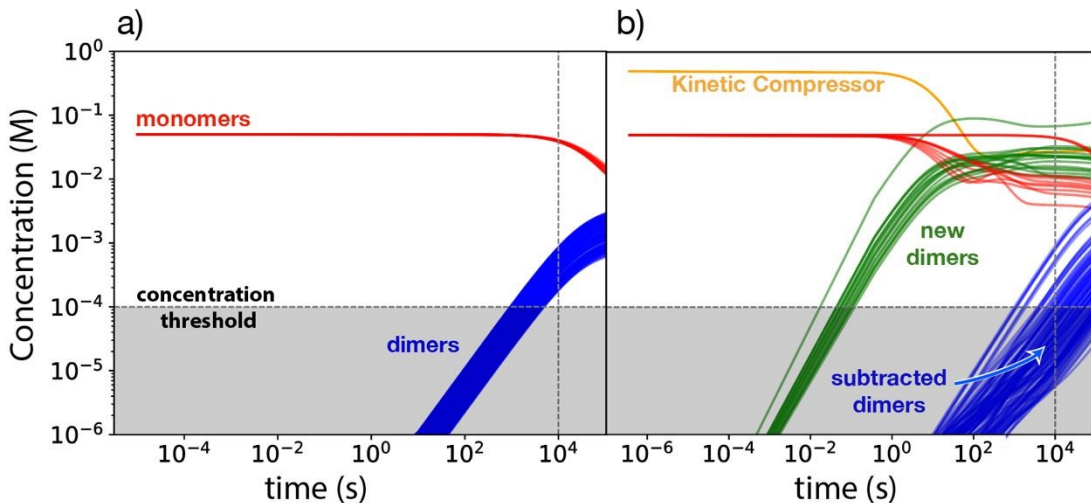


**Figure 6.** Time evolution of monomer (red lines) and dimer (blue lines) concentrations in the (a) absence of a kinetic compressor and (b) presence of a kinetic compressor (orange line). All monomers are fully connected except for the kinetic compressor, which is partially connected, meaning that it can only react with a subset of monomers. Dimers that contain the kinetic compressor form quickly (green lines). Dimers that do not contain the kinetic compressor form slowly (blue lines). The kinetic compressor delays the rise of some products (subtracted products in b). The vertical dashed line indicates the time point at which measurements are made. Parameters for this simulation are indicated in Table 1.

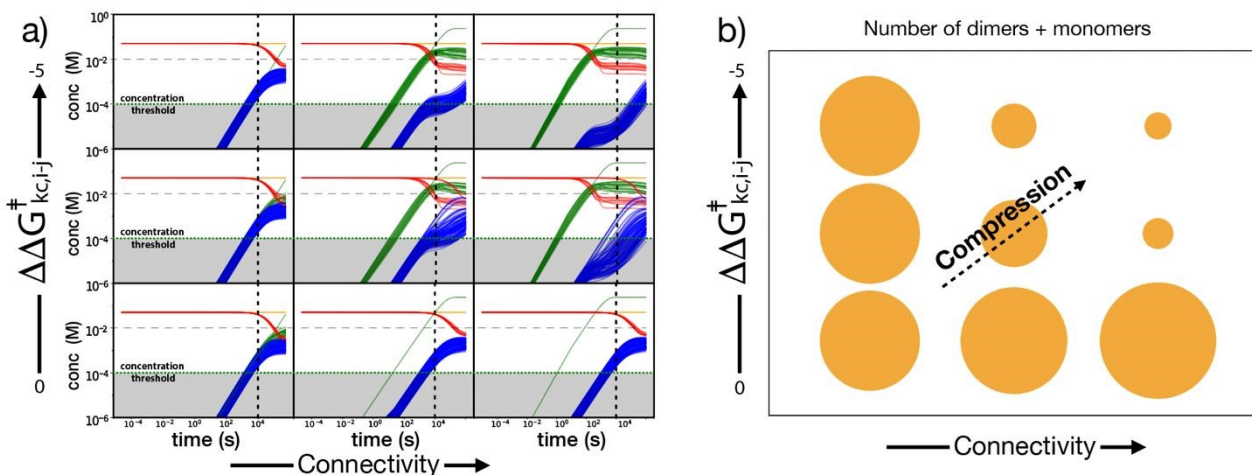


**Figure 7.** Effects of connectivity and  $\Delta\Delta G^\ddagger$  on the reaction of monomers to dimers. The number of dimers and monomers above the concentration threshold at time=1000s is determined by chemical connectivity and  $\Delta\Delta G^\ddagger$ . a) Chemical connectivity of the compressor is varied from isolated, to partially connected (the kinetic compressor reacts with 3 out of 12 monomers), to fully connected (the kinetic compressor reacts with 12 of 12 monomers). The  $\Delta\Delta G^\ddagger$  of the kinetic compressor varies from 0 kcal/mol (no compression), to -3 kcal/mol, to -5 kcal/mol (strong compression). The time point at which concentrations are determined is indicated by a vertical dashed line at time=1000s. b) A summary showing how concentrations of dimers are influenced by connectivity and  $\Delta\Delta G^\ddagger$ . Parameters for this simulation are indicated in Table 1 except for variation of  $\Delta\Delta G^\ddagger$  and connectivity of the compressor. The concentration of kinetic compressor is kept constant at 0.05M through feeding.

The balance between combinatorial compression and explosion depends on chemical connectivity,  $\Delta\Delta G^\ddagger$ , concentrations, time, and temperature. Figure 7 shows that when  $\Delta\Delta G^\ddagger$  is close to zero and connectivity is low, all dimers rise above the concentration threshold, even at low temperature. In this exploded state, 12 reactants combine to form 144 dimers. By contrast, when  $\Delta\Delta G^\ddagger$  is large in magnitude and connectivity is high, many dimers remain below threshold. In this compressed state, 12 monomers,



including the kinetic compressor, form only 23 dimers. Kinetic compression is observed only when the system is under kinetic control and is pronounced at relatively low temperatures and short reaction times. Indeed, our previous experiments demonstrate that modest increases in temperature cause the number of products to explode (12).

### Combinatorial Compression under Thermodynamic Control

Here we describe simulations of combinatorial compression in connected systems at equilibrium. A thermodynamic compressor ( $M_{tc}$ ), must be highly connected, at high concentration, and have a free energy of reaction ( $\Delta G_{rxn}$ ) greater in magnitude than the free energies of reaction of other monomers ( $\Delta \Delta G_{rxn} \approx -1$  to  $-8$  kcal/mol, Figure 8a). Hence, the reaction of the thermodynamic compressor has greater driving force than the reactions of other monomers (20-23).

In our equilibrium simulations, the  $\Delta H^\circ$  for reactions between monomers is 8 kcal/mol, except for reactions involving the thermodynamic compressor, for which it is 0 kcal/mol (Figure 8a). The  $\Delta S^\circ$  is 0.033 kcal/mol•K for all reactions.  $\Delta G = \Delta H^\circ - T\Delta S^\circ$  at 40°C is -10.4 kcal/mol for reactions with the thermodynamic compressor and -2.4 kcal/mol for all other reactions. The value of  $\Delta G(rxn)$  changes over the course of the reaction as concentrations of reactants and products change, but is generally slightly less than  $\Delta G$ :  $\Delta G(rxn) = \Delta G - RT \ln\left(\frac{[D_{ij}][W]}{[M_i][M_j]}\right) \approx -10.82$  kcal/mol for the thermodynamic compressor and  $\approx -2.82$  kcal/mol for all other dimerization reactions. Other reaction conditions are specified in Table 1. The balance between compression and explosion at equilibrium depends on reaction free energies (Figure 8a), concentrations (Figure 8b), and chemical connectivity (Figure 8c and 8d). Figure 8d shows that increasing connectivity or increasing the magnitude of  $\Delta \Delta G_{rxn}$  of one monomer causes the number of detectable dimers to decrease from 144 to 23. Thermodynamic compression requires relatively high temperatures or long reaction times.



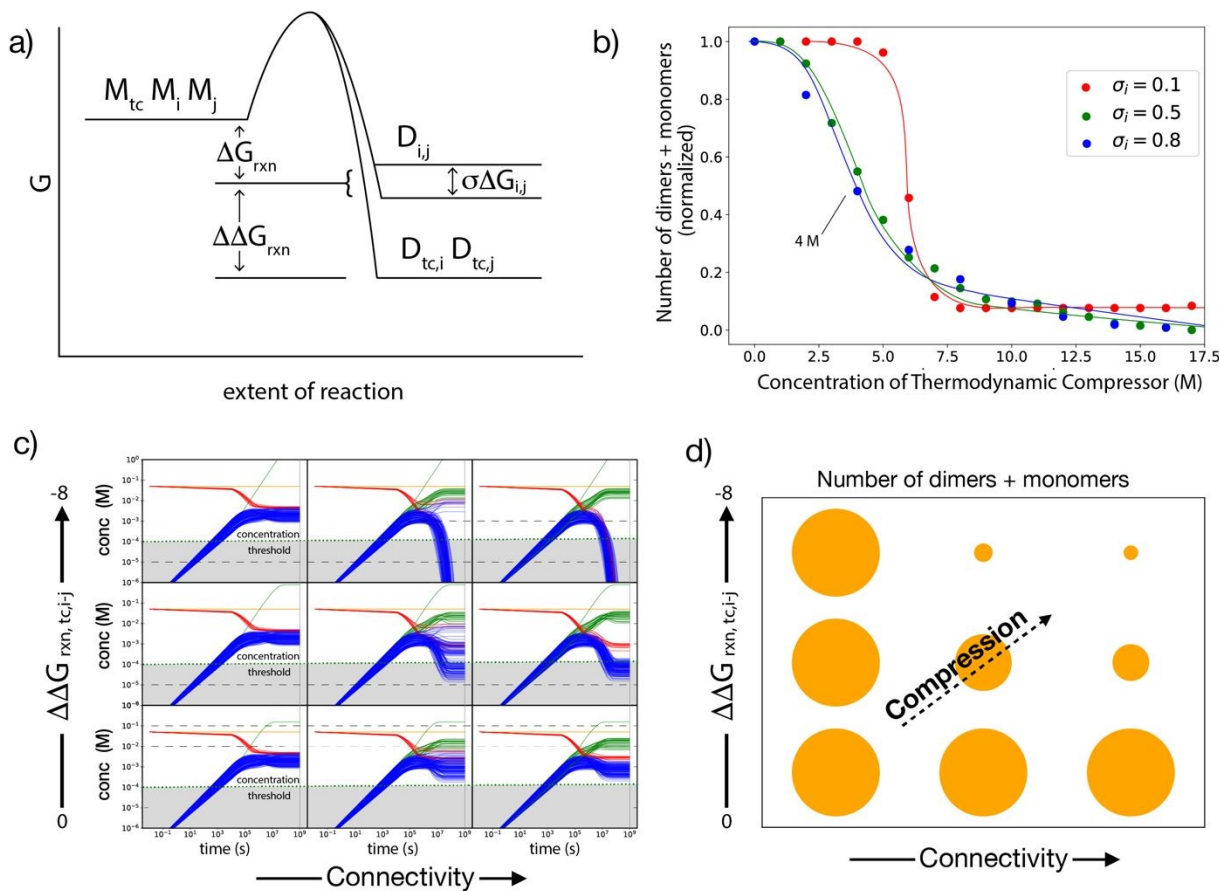


**Figure 8.** Effect of connectivity **and**  $\Delta\Delta G_{rxn}$  in the reaction of monomers to dimers. a) A schematic of a reaction coordinate indicating relative free energies of reaction for  $M_i + M_j \rightarrow D_{i,j}$  and  $M_i + M_{tc} \rightarrow D_{i,tc}$ , where  $M_{tc}$  is the thermodynamic compressor. b) The number of dimers and monomers above the concentration threshold at equilibrium depends on the concentration of the thermodynamic compressor and the standard deviation of the free energies of reaction. Parameters for this simulation are as indicated in Table 1, except the standard deviation in free energies of reaction, which is set to three different values:  $\sigma_i(\Delta G_{rxn}) = 0.043$  (red line), 0.213 (green), or 0.340 (blue) kcal/mol. The time interval is  $10^9$  seconds, which allows equilibrium. Results are normalized from 0 to 1; values reaching the minimum appear as zero. c) Changes in concentrations of dimers over time and at equilibrium are influenced by connectivity and  $\Delta\Delta G_{rxn}$ . Chemical connectivity varies from isolated, to ‘partially connected’ in which the thermodynamic compressor is connected to 3 out of 12 monomers, to fully connected. The  $\Delta G_{rxn}$  for reactions of the thermodynamic compressor vary from -2.82 kcal/mol ( $\Delta\Delta G_{rxn} = 0$  kcal/mol), to -3.82 kcal/mol ( $\Delta\Delta G_{rxn} = -1$  kcal/mol), to -10.82 kcal/mol ( $\Delta\Delta G_{rxn} = -8$  kcal/mol). The concentration of the thermodynamic compressor is held constant at 0.05 M. d) The number of dimers and monomers above the concentration threshold is determined by  $\Delta\Delta G_{rxn}$  and chemical connectivity of the compressor. The concentration of thermodynamic compressor is kept constant at 0.05M through feeding in c) and d).

In comparison to kinetic control, in thermodynamic control the transition from combinatorial explosion to compression requires a higher concentration of compressor. In the kinetics simulation, the transition from explosion to compression occurs with an initial concentration of kinetic compressor of around 10 times the concentration of other monomers (Figure 4). In the thermodynamics simulation, the transition from explosion to compression occurs at an initial concentration of the thermodynamic compressor of around 100 times the concentration of other monomers (5 M, Figure 8b). In both the kinetic and thermodynamic realms, the number of products varies inversely with the concentration of the compressor. In the simulations in Figure 8c and 8d, the thermodynamic compressor is fed to the reaction continuously, such that it is maintained at a constant concentration as it is consumed by the reactions. This



protocol is followed to avoid the high concentrations of thermodynamic compressor required for compression, which gives a kinetic advantage to the thermodynamic compressor that obscures the true effect of a thermodynamic compression.

Thermodynamic and kinetic compression have fundamentally different origins and are observed under strikingly different conditions; thermodynamic control for thermodynamic compression versus kinetic control for kinetic compression. Kinetic compression appears to be more relevant than thermodynamic compression to selection during chemical evolution, according to recent experiments (12).

### Systems with both Kinetic and Thermodynamic Compression.

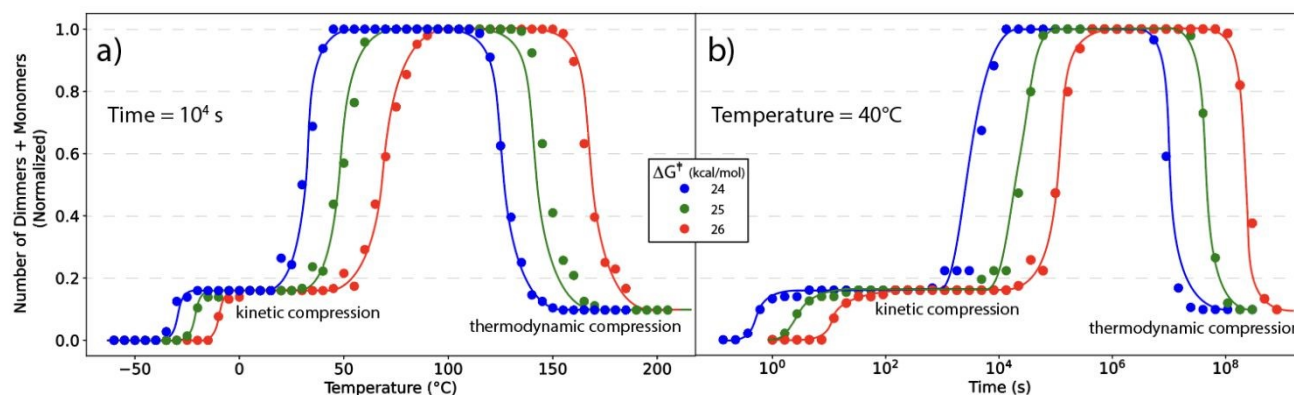


**Figure 9.** Combined Kinetic and Thermodynamic Compression. a) Normalized number of monomers plus dimers versus temperature at constant time of 10,000 seconds. b) Normalized number of monomers plus dimers versus time at constant temperature of  $40^\circ\text{C}$ . Both panels show transitions from kinetic combinatorial compression to explosion to thermodynamic compression. The concentrations of both kinetic and thermodynamic compressors are constant at 0.05 M. Mean activation free energies are 26 kcal/mol (21) (red lines), 25 kcal/mol (20) (green lines), and 24 kcal/mol (19) (blue lines). Other parameters for these simulations are indicated in Table 1.

To understand how temperature and time in combination affect combinatorial compression, we simulated evolution of a combined system with both kinetic and thermodynamic compression. These simulations employed both a kinetic and a thermodynamic compressor. The two compressors are distinct monomers. Monomers in the systems are fully connected. Feeding (continuous addition) maintained constant concentration of both the kinetic and the thermodynamic compressors (Figures 9-10). The simulations show that the mixture is kinetically compressed at low temperature, under kinetic control, with under 20% of the normalized monomers and dimers above the threshold after a given time interval. The system is combinatorically exploded at intermediate temperatures, with 100% of possible monomers and dimers over the concentration threshold. The system is thermodynamically compressed at high temperatures, under thermodynamic control, with under 18% of the normalized monomers and dimers over the concentration threshold (Figure 9a). A set of dimers dominates the reaction under kinetic control. A different set of dimers dominates the system under thermodynamic control. Combinatorial compression at low temperatures produced dimers containing the kinetic compressor. Combinatorial compression at high temperatures produces dimers containing the thermodynamic compressor. No single dimer dominates the mixture in both realms. These compositions are confirmed by independent simulations of a system with only a thermodynamic compressor, in which combinatorial compression is observed only at high temperatures, and simulations of a system with only kinetic compressor, in which combinatorial compression is observed only at low temperatures (Figure S2). At a fixed temperature, the system

transitions over time from kinetic compression to combinatorial explosion to thermodynamic compression (Figure 9b). The balance between combinatorial compression and explosion is dependent on the reaction time, in a manner similar to the temperature (Figure 9a). However, this relationship may not hold for reactions in which entropy makes a major contribution to the free energy of reactions, or when enthalpy and entropy exhibit strong temperature dependence.

The temperature and reaction time of the transition from combinatorial compression to explosion in the combined system are dependent on the activation energies of the chemical reactions in the mixture (Figure 9). For higher activation energies, higher temperatures or longer reaction times are required to observe the kinetic-related transition and the thermodynamic-related transition. The slope of the transition in Figure 9 depends on the variability in activation energies and enthalpies (Figure S2).

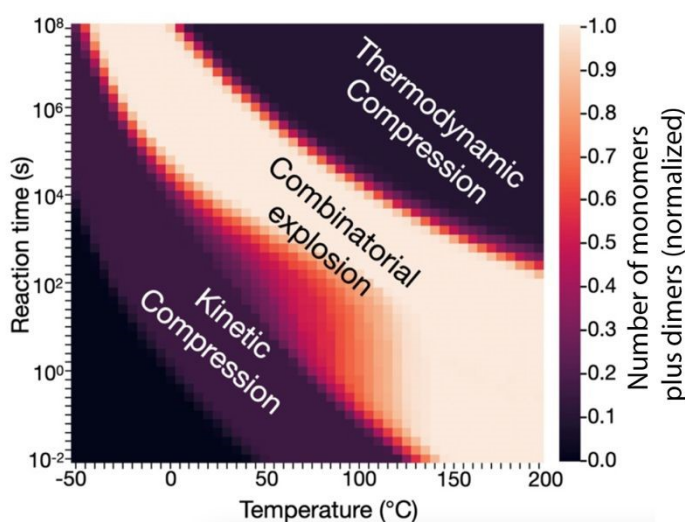


**Figure 10.** Normalized number of monomers and dimers as a function of the temperature and reaction time. Three states are identified: Thermodynamic compression, combinatorial explosion, kinetic compression. In addition, at very short reaction times and low temperatures, we observe the case in which initial components do not react significantly and persist over the course of the simulation. Parameters for this simulation are set as in Table 1, except for the concentrations of both kinetic and thermodynamic compressors are constant at 0.05 M. Temperature ranges from -50°C to 200°C, reaction times range from 10<sup>-2</sup>s to 10<sup>8</sup>s.

Giving the system either more time to react or increasing the temperature can drive a system from kinetic compression to combinatorial explosion, followed by a thermodynamic compression. Figure 10 shows plot of normalized number of monomers and dimers as a function of the reaction time and temperature realms of kinetic compression, combinatorial explosion, and thermodynamic compression. The pseudo-symmetry across the diagonal (from top-left to bottom-right) indicates a rough equivalence of the effects of temperature and reaction time. There are subtle but important distinctions between the effects of reaction time and the effects of temperature. A linear increase in temperature is equivalent to an exponential increase in reaction time (see the logarithmic scale of the reaction time axis in Figures 9-10). Moreover, at sufficiently low temperatures, some reactions do not occur for thermodynamic reasons. There is no combinatorial explosion at very low temperatures (Figure 10). This behavior has no equivalence in reaction times; decreasing reaction times cannot affect the driving force (thermodynamics) of the reaction.

Thermodynamic compression is independent of initial conditions. However, kinetic compression requires initial conditions with monomers only, or semi-continuous dissociation of dimers (such as hydrolysis through dry-wet cycling) or feeding with new monomers. We plot the dependence of the states



identified in Figure 10 as a function of the number of monomer types included in the mixture, the concentration threshold for dimers, and the variability in free activation energies and enthalpies (Figure S3). In all cases, we identify the states of combinatorial explosion, kinetic and thermodynamic compression. The transitions between these states are sharper for small variability of activation energies and enthalpies. The state of explosion is more pronounced for a low concentration threshold. In addition, we plot the dependence of the thermodynamic and kinetic compression on the initial concentration of reactants (Figure S4). It is evident that thermodynamic compression is independent of initial concentrations whereas kinetic compression is dependent.

## Discussion

*Combinatorial Compression under Kinetic Control.* Using basic chemical principles and simulations, we have recapitulated experimental phenomena characteristic of chemical evolution. Stringent selection and compression under kinetic control are characterized by: (i) production of fewer products than expected from the combinatorics of the reactants; (ii) loss of some products upon addition of new reactants; and (iii) temperature-dependent transitions between compression and explosion. These simulations of a single drying step are consistent with acute selection based on reaction kinetics within complex chemical ensembles. We can now explain underlying principles of chemical selection and combinatorial compression. The simulations indicate that selection and combinatorial compression under kinetic control require:

- Connection. Many reactants must form chemical connections to many other reactants.
- High reactivity. One (or a few) reactants must be more reactive and at sufficient concentration and react faster than others.
- Temperature. The temperature must be appropriate to the activation energies and the reaction time.

The results are relevant to known condensation–dehydration reactions. Mixtures of mercapto acids, hydroxy acids, and amino acids form highly connected systems and react to form thioester, ester, and amide bonds, with activation free energies in the range of 20–35 kcal/mol. These reactions are favorable during drying (5–13).

The results of the simulations are general and are not dependent on specific chemical identities. Kinetic compression depends on activation energies, concentrations, connection, time and temperature. For example, a reactant with  $\Delta G^\ddagger = 20$  kcal/mol might be kinetically dominant in a mixture with other reactants with  $\Delta G^\ddagger = 25$  kcal/mol but not in a mixture with reactants with  $\Delta G^\ddagger = 20$  kcal/mol. A reactant at 0.25 M can act as a kinetic compressor if the sum of other concentrations is 0.1 M, but not if the sum of other concentrations is 0.5 M. A kinetically dominant reactant with  $\Delta G^\ddagger = 20$  kcal/mol causes combinatorial compression at 45°C while a dominant reactant with  $\Delta G^\ddagger = 30$  kcal/mol would cause combinatorial compression at a higher temperatures and/or longer reaction times.

Given sufficient time, a kinetically compressed system can combinatorially explode. However, kinetic compression can persist indefinitely, if a system is prevented from reaching equilibrium. Continuously changing conditions can preclude equilibrium. Wet-dry cycling, feeding of reactants, and formation of kinetically trapped products can prevent equilibrium.

*Chemical Evolution and Stringency of Selection.* Selection during wet–dry cycling can be remarkably stringent, imposing sharp constraints on reaction trajectories under specific physicochemical conditions. In particular, complex chemical systems that combine cyclic environmental forcing with appropriate kinetic asymmetries can sustain high concentrations of selected products over time and, as a



result, evolve chemically. While such stringent selection does not arise across the full parameter space, our results indicate that it emerges robustly within a defined and physically plausible subset of conditions, suggesting that chemical selection and combinatorial compression may represent necessary ingredients for chemical evolution.

Our experiments and simulations indicate that small differences in activation free energies can control and direct product formation. We find that a modest difference of just 3 kcal/mol, equivalent to approximately five times the thermal energy at 40 °C, is sufficient to direct and focus the flow of chemical reactions. Under the conditions of the dry phase, where condensation reactions dominate, small energetic differences can sculpt the kinetic landscape, resulting in distinct and reproducible product distributions.

The combined results suggest that production of certain products in complex chemical systems is possible from real-time selection based on inherent chemical properties and environmental conditions. Complex chemical systems are sensitive to internal and external parameters in the absence of enzymes or other mechanisms of biological control. The dry phase of wet-dry cycling acts as a stringent kinetic filter, favoring synthetic pathways with the lowest effective activation barriers. Minimal differences in reactivity can be magnified into large differences in chemical outcomes, contributing to the selectivity.

We hypothesize that additional selective pressures, acting in concert with kinetic compression, contributed to the emergence of complex oligomers and polymers during the origins of life (26). The data support a model in which molecular ensembles evolve in response to dynamic, continuously shifting selective pressures (12, 27). Selection during wet-dry cycling can involve: solubility in water (wet phase); intrinsic condensation kinetics (dry phase); resistance to hydrolysis (wet phase); catalytic enhancement of condensation, such as through ester–amide exchange (dry phase) (10, 11, 28); molecular recalcitrance (wet phase) (1, 29); and, ultimately, autocatalytic cycles (30, 31). In this model, kinetic trapping during the dry phase can drive the formation of large molecules. As the complexity of individual molecules increases, additional selective forces are likely to emerge, including deep kinetic traps formed by recalcitrant assemblies (29) and the development of autocatalytic behavior (30, 31).

The results of our simulations here can guide the design of new experiments concerning chemical evolution. It appears that conditions expected on the early Earth can enable kinetic compression and chemical evolution. Moreover, we believe that kinetic compression is a universal phenomenon that might have broad implications in chemical and related fields.

An acute culling of chemical diversity occurred during the transition from abiotic chemistry to biochemistry. Abiotic chemical systems exhibit far greater molecular diversity than biochemical systems (2, 32). During the origins of life, a net decrease in the overall chemical diversity of the evolving ensemble was accompanied by an increase in the size and complexity of individual molecules. Combinatorial compression, based on selection operating during the kinetics of condensation reactions, may have served as a key mechanism for molecular culling during the origins of life. Other compressive phenomena include the action of borate (33), and the effect of metal ions and minerals (34-37) and the convergence to a single genetic code (38).

*Combinatorial Compression under Thermodynamic Control.* In addition to kinetic compression, in this work we identified a phenomenon we call thermodynamic compression, based on selection on thermodynamics of reaction. In this realm the most stable products are selected over other products.

A system that is thermodynamically compressed, does not explore new chemical spaces and does not undergo chemical evolution. Thermodynamic compression does not explain the experiments in (12),



and it is reasonable to assume that it did not drive prebiotic chemical evolution because: (i) life is far from equilibrium, (ii) equilibrium has intrinsic ‘sink-like’ behavior that challenges continuous chemical change (39), and (iii) long times are required to reach a thermodynamic compression.

Kinetic and thermodynamic compression are fundamentally different phenomena, driven by different factors and occurring on different timescales. Kinetic compression arises under short reaction times or when the system is coupled to processes (e.g., dry–wet cycling) that prevent it from reaching equilibrium. In contrast, thermodynamic compression requires prolonged reaction times and occurs as a system approaches equilibrium. Kinetic compression is a transient state that emerges before the full set of possible products is realized, whereas thermodynamic compression reflects a distribution at equilibrium.

Combinatorial compression reflects chemical selection of few products from a large possibility space. In prior work, chemical selection has been observed across multiple scales by various mechanisms. Examples of systems that harvest environmental energy and invest it in chemical reactions include *in vivo* biochemistry and *in vitro* condensation reactions in wet–dry cycling conditions. Wet–dry cycling uses kinetic control and energy dissipation to select for complex oligomers (12, 13). Similarly, stellar nucleosynthesis selects for stable configurations of protons and neutrons (40). Mineral evolution selects for locally stable arrangements of chemical elements (41). Biology uses Darwinian evolution to select for persistent arrangements of fragile organic molecules.

## Data availability

The Python code developed to perform computer simulations of this work can be found at: <https://github.com/HUJI-MFP/Compression/tree/main>. Using this code, all results shown in this manuscript are reproducible.

## Author contributions

PCA, LDW, and MFP conceptualized the research. Computer simulations were conducted by PCA. ASP and YP contributed to improving the organization and clarity of the code. The manuscript was written and edited by all authors. All authors have approved the final version of the manuscript.

## Conflicts of interest

There are no conflicts to declare.

## Acknowledgments

We thank Prof. Doron Lancet for helpful discussions. This research was funded by the European Union to MFP (ERC, Sweet\_Evo, 101163270), the Azrieli Foundation Early Career Faculty Grant, the Israel Science Foundation grant (1611/22), the Minerva Foundation, the FEBS Foundation Excellence Award to MFP, and the National Aeronautics Space Agency Grant no. 80NSSC24K0344. Views and opinions expressed are however those of the author only and do not necessarily reflect those of the European Union or the European Research Council. Neither the European Union nor the granting authority can be held responsible for them.



## References

1. Matange K, Marland E, Frenkel-Pinter M, Williams LD. Biological Polymers: Evolution, Function, and Significance. *Acc Chem Res.* 2025;3137–610.
2. Nelson DL, Lehninger AL, Cox MM. *Principles of Biochemistry*, 8th Edition: Macmillan; 2021.
3. Mamajanov I, MacDonald PJ, Ying J, Duncanson DM, Dowdy GR, Walker CA, et al. Ester formation and hydrolysis during wet–dry cycles: generation of far-from-equilibrium polymers in a model prebiotic reaction. *Macromolecules.* 2014;47(4):1334–43.
4. Damer B, Deamer D. The hot spring hypothesis for an origin of life. *Astrobiology.* 2020;20(4):429–52.
5. Yu S-S, Solano MD, Blanchard MK, Soper-Hopper MT, Krishnamurthy R, Fernández FM, et al. Elongation of model prebiotic proto-peptides by continuous monomer feeding. *Macromolecules.* 2017;50(23):9286–94.
6. Li Z, Li L, McKenna KR, Schmidt M, Pollet P, Gelbaum L, et al. The oligomerization of glucose under plausible prebiotic conditions. *Orig Life Evol Biosph.* 2019;49(4):225–40.
7. Rodriguez-Garcia M, Surman AJ, Cooper GJ, Suárez-Marina I, Hosni Z, Lee MP, et al. Formation of oligopeptides in high yield under simple programmable conditions. *Nat Commun.* 2015;6(1):8385.
8. Frenkel-Pinter M, Haynes JW, Petrov AS, Burcar BT, Krishnamurthy R, Hud NV, et al. Selective incorporation of proteinaceous over nonproteinaceous cationic amino acids in model prebiotic oligomerization reactions. *Proc Natl Acad Sci USA.* 2019;116(33):16338–46.
9. Jia TZ, Caudan M, Mamajanov I. Origin of species before origin of life: the role of speciation in chemical evolution. *Life.* 2021;11(2):154.
10. Forsythe JG, Yu SS, Mamajanov I, Grover MA, Krishnamurthy R, Fernández FM, et al. Ester-mediated amide bond formation driven by wet–dry cycles: A possible path to polypeptides on the prebiotic earth. *Angew Chem Int Ed.* 2015;54(34):9871–5.
11. C M, Frenkel-Pinter M, Smith KH, Rivera-Santana VF, Sargon AB, Jacobson KC, et al. Water-Based Dynamic Depsipeptide Chemistry: Building Block Recycling and Oligomer Distribution Control Using Hydration–Dehydration Cycles. *JACS Au.* 2022;2(6):1395.
12. Matange K, Rajaei V, Capera-Aragones P, Costner JT, Robertson A, Kim JS, et al. Evolution of complex chemical mixtures reveals combinatorial compression and population synchronicity. *Nat Chem.* 2025;17:590–59.
13. Forsythe JG, Petrov AS, Millar WC, Yu SS, Krishnamurthy R, Grover MA, et al. Surveying the sequence diversity of model prebiotic peptides by mass spectrometry. *Proc Natl Acad Sci U S A.* 2017;114(37):E7652–E9.
14. Li Z, Sim CH, Low MYH, editors. *A survey of emergent behavior and its impacts in agent-based systems.* 2006 4th IEEE international conference on industrial informatics; 2006: IEEE.
15. Nogal N, Sanz-Sánchez M, Vela-Gallego S, Ruiz-Mirazo K, de la Escosura A. The protometabolic nature of prebiotic chemistry. *Chemical Society Reviews.* 2023.
16. Asche S, Cooper GJT, Keenan G, Mathis C, Cronin L. A robotic prebiotic chemist probes long term reactions of complexifying mixtures. *Nat Commun.* 2021;12(1):3547.
17. Guttenberg N, Virgo N, Chandru K, Scharf C, Mamajanov I. Bulk measurements of messy chemistries are needed for a theory of the origins of life. *Philos Trans R Soc London, Ser A.* 2017;375(2109):20160347.
18. Orgel LE. Prebiotic chemistry and the origin of the RNA world. *Crit Rev Biochem Mol Biol.* 2004;39(2):99–123.
19. Schuster P. Taming combinatorial explosion. *Proc Natl Acad Sci USA.* 2000;97(14):7678–80.
20. Corbett PT, Leclaire J, Vial L, West KR, Wietor J-L, Sanders JK, et al. Dynamic combinatorial chemistry. *Chem Rev.* 2006;106(9):3652–711.
21. Cao Y, Yang J, Eichin D, Zhao F, Qi D, Kahari L, et al. Self-synthesizing nanorods from dynamic combinatorial libraries against drug resistant cancer. *Angew Chem Int Ed.* 2021;60(6):3062–70.
22. Lei Z, Chen H, Huang S, Wayment LJ, Xu Q, Zhang W. New advances in covalent network polymers via dynamic covalent chemistry. *Chem Rev.* 2024;124(12):7829–906.
23. Sood A, Mandal PK, Ottelé J, Wu J, Eleveld M, Hatai J, et al. Simultaneous Formation of a Foldamer and a Self-Replicator by Out-of-Equilibrium Dynamic Covalent Chemistry. *J Am Chem Soc.* 2024;146(49):33386–94.



24. Yu S-S, Krishnamurthy R, Fernández FM, Hud NV, Schork FJ, Grover MA. Kinetics of prebiotic depsipeptide formation from the ester–amide exchange reaction. *Phys Chem Chem Phys*. 2016;18(41):28441–50.

25. Higgs PG. The effect of limited diffusion and wet–dry cycling on reversible polymerization reactions: implications for prebiotic synthesis of nucleic acids. *Life*. 2016;6(2):24.

26. Ashkenasy G, Hermans TM, Otto S, Taylor AF. Systems chemistry. *Chemical Society Reviews*. 2017;46(9):2543–54.

27. Matange K, Rajaei V, Schuster G, Hud NV, Menor-Salvan C, Capera-Aragonès P, et al. Origins of Life: Chemistry and Evolution. *Nature Chemistry* (second round review). 2025;10.26434/chemrxiv–2023–1jrcq–v2.

28. Frenkel-Pinter M, Bouza M, Fernández FM, Leman LJ, Williams LD, Hud NV, et al. Thioesters provide a plausible prebiotic path to proto-peptides. *Nat Commun*. 2022;13(1):2569.

29. Edri R, Fisher S, Menor-Salvan C, Williams LD, Frenkel-Pinter M. Assembly-Driven Protection from Hydrolysis as Key Selective Force during Chemical Evolution. *FEBS Lett*. 2023.

30. Hordijk W, Hein J, Steel M. Autocatalytic sets and the origin of life. *Entropy*. 2010;12(7):1733–42.

31. Vincent L, Berg M, Krismer M, Saghafi ST, Cosby J, Sankari T, et al. Chemical ecosystem selection on mineral surfaces reveals long-term dynamics consistent with the spontaneous emergence of mutual catalysis. *Life*. 2019;9(4):80.

32. Glavin DP, Dworkin JP, Alexander CMOD, Aponte JC, Baczynski AA, Barnes JJ, et al. Abundant ammonia and nitrogen-rich soluble organic matter in samples from asteroid (101955) Bennu. *Nature Astronomy*. 2025;1–12.

33. Benner S. Borate Minerals Stabilize Ribose. *Science*. 2004;303:196.

34. Colón-Santos S, Cooper GJ, Cronin L. Taming the combinatorial explosion of the formose reaction via recursion within mineral environments. *ChemSystemsChem*. 2019;1(3):e1900014.

35. Chandru K, Potiszil C, Jia TZ. Alternative Pathways in Astrobiology: Reviewing and Synthesizing Contingency and Non-Biomolecular Origins of Terrestrial and Extraterrestrial Life. *Life*. 2024;14(9):1069.

36. Hazen RM, Filley TR, Goodfriend GA. Selective adsorption of L-and D-amino acids on calcite: Implications for biochemical homochirality. *Proc Natl Acad Sci USA*. 2001;98(10):5487–90.

37. Surman AJ, Rodriguez-Garcia M, Abul-Haija YM, Cooper GJ, Gromski PS, Turk-MacLeod R, et al. Environmental control programs the emergence of distinct functional ensembles from unconstrained chemical reactions. *Proc Natl Acad Sci USA*. 2019;116(12):5387–92.

38. Vetsigian K, Woese C, Goldenfeld N. Collective evolution and the genetic code. *Proc Natl Acad Sci USA*. 2006;103(28):10696–701.

39. Benner SA, Kim H-J, Carrigan MA. Asphalt, water, and the prebiotic synthesis of ribose, ribonucleosides, and RNA. *Acc Chem Res*. 2012;45(12):2025–34.

40. Wong ML, Cleland CE, Arend Jr D, Bartlett S, Cleaves HJ, Demarest H, et al. On the roles of function and selection in evolving systems. *Proc Natl Acad Sci USA*. 2023;120(43):e2310223120.

41. Hazen RM, Ferry JM. Mineral evolution: Mineralogy in the fourth dimension. *Elements*. 2010;6(1):9–12.



**Data availability** The Python code developed to perform computer simulations of this work can be found at: <https://github.com/HUJI-MFP/Compression/tree/main>. Using this code, all results shown in this manuscript are reproducible.

